Article

Membrane Lipids Tune Synaptic Transmission by Direct Modulation of Presynaptic Potassium Channels

Mario Carta,[1,4] Frederic Lanore,[1,4] Nelson Rebola,[1,4] Zsolt Szabo,[1] Silvia Viana Da Silva,[1] Joana Lourenço,[1] Agathe Verraes,[3] André Nadler,[2] Carsten Schultz,[2] Christophe Blanchet,[1] and Christophe Mulle[1,*]

[1]University of Bordeaux, Interdisciplinary Institute for Neuroscience, CNRS UMR 5297, 33000 Bordeaux, France
[2]EMBL Heidelberg, Meyerhofstraße 1, 69117 Heidelberg, Germany
[3]Institut Jacques Monod, UMR 7592, CNRS and INSERM ERL U950, University Paris Diderot, Sorbonne Paris Cité, 75013 Paris, France
[4]These authors contributed equally to this work
*Correspondence: christophe.mulle@u-bordeaux.fr
http://dx.doi.org/10.1016/j.neuron.2013.12.028

SUMMARY

Voltage-gated potassium (Kv) channels are involved in action potential (AP) repolarization in excitable cells. Exogenous application of membrane-derived lipids, such as arachidonic acid (AA), regulates the gating of Kv channels. Whether membrane-derived lipids released under physiological conditions have an impact on neuronal coding through this mechanism is unknown. We show that AA released in an activity-dependent manner from postsynaptic hippocampal CA3 pyramidal cells acts as retrograde messenger, inducing a robust facilitation of mossy fiber (Mf) synaptic transmission over several minutes. AA acts by broadening presynaptic APs through the direct modulation of Kv channels. This form of short-term plasticity can be triggered when postsynaptic cell fires with physiologically relevant patterns and sets the threshold for the induction of the presynaptic form of long-term potentiation (LTP) at hippocampal Mf synapses. Hence, direct modulation of presynaptic Kv channels by activity-dependent release of lipids serves as a physiological mechanism for tuning synaptic transmission.

INTRODUCTION

Synaptic transmission mainly flows anterogradely from the action-potential-dependent release of neurotransmitters to the activation of specific postsynaptic membrane receptors. Many neurons can also modulate the strength of their synaptic inputs through the release of retrograde messengers (Regehr et al., 2009). Retrograde messengers, including membrane-derived lipids, gases, peptides, growth factors, or conventional neurotransmitters, can be released from postsynaptic neurons in response to activity and diffuse to presynaptic terminals where they interact with specific targets in order to regulate neurotransmitter release (Regehr et al., 2009). In the CNS, most of the reported lipid-mediated retrograde modulation of synaptic transmission involves endocannabinoids and cannabinoid type 1 receptors (CB1Rs) (Wilson and Nicoll, 2002), which are present in both GABAergic and glutamatergic neurons (Herkenham et al., 1990; Kawamura et al., 2006; Marsicano and Lutz, 2006). Postsynaptic calcium rise leads to the production of endogenous lipids (2-AG and anandamide), which diffuse into the presynaptic terminal and activate CB1Rs, leading to the inhibition of neurotransmitter release (Kano et al., 2009; Marsicano and Lutz, 2006). Other membrane receptors activated by lipids, such as transient receptor potential cation channel subfamily V member 1 (TRPV1) and lysophosphatidic acid receptor 2 receptors, have also been reported to modulate synaptic transmission (Gibson et al., 2008; Trimbuch et al., 2009).

Apart from their action through specific membrane receptors, membrane-derived lipids are also known to modulate ion channel function by direct interaction with the ion channel (Boland and Drzewiecki, 2008). Lipids are known to modulate voltage-dependent calcium channels (Roberts-Crowley et al., 2009), potassium channels (Oliver et al., 2004), glycine receptors (Lozovaya et al., 2005), and GABA_A receptors (Sigel et al., 2011). Membrane-derived lipids may also represent the primary activating ligands of TRP channels (Hardie, 2007; Kukkonen, 2011) or two-pore domain potassium channels (Besana et al., 2005). However, contrasting with the large number of reports on direct modulation of ion channels by membrane-derived lipids, the physiological conditions under which this mechanism is recruited remains elusive.

To address this question, we focused on hippocampal mossy fiber (Mf) CA3 synapses. The efficacy of Mf-CA3 synaptic transmission is tightly controlled by presynaptic Kv channels, and Mf-CA3 presynaptic terminals are amenable to patch-clamp recordings (Geiger and Jonas, 2000). We have identified a retrograde signaling mechanism which results in robust short-term potentiation of synaptic transmission in physiological conditions of activity of hippocampal circuits. This potentiation is mediated by the activation of phospholipase A2 and the release of arachidonic acid (AA) and is not dependent on any known membrane lipid receptor. Using patch-clamp recordings from
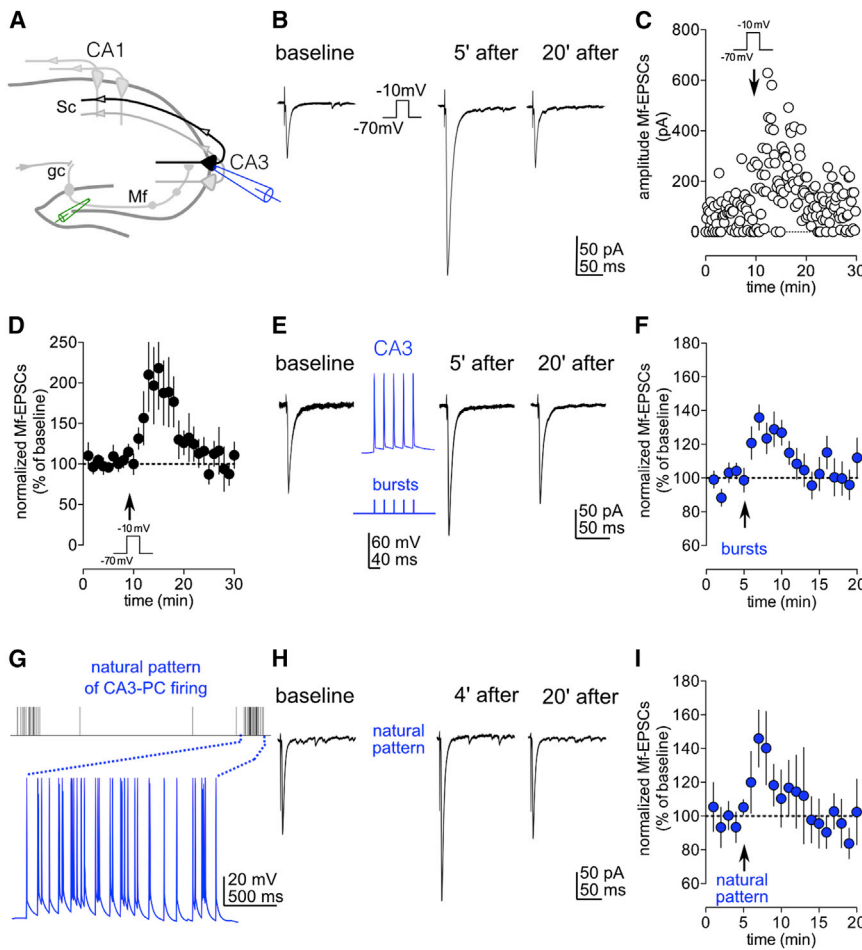
Figure 1. Postsynaptic Depolarization or Postsynaptic Action Potential Firing Induces Potentiation at Mf-CA3 Synaptic Transmission

(A) Illustration of a hippocampal slice with recording (blue, in a CA3 pyramidal cell) and stimulating electrodes (green, inside the dentate gyrus).

(B) Sample traces (average of 30 sweeps) of Mf-EPSCs before and 5′ or 20′ after the depolarization step (from −70 to −10 mV).

(C) Time course of amplitudes of individual Mf-EPSCs recorded in the same cell as in (B).

(D) Summary time course of normalized Mf-EPSCs for experiments illustrated in (B) and (C) (n = 12).

(E) DPE of Mf-EPSCs can be induced by a burst of APs at theta frequency (bursts of five APs delivered at 25 Hz, repeated six times every 140 ms).

(F) Summary time course of normalized Mf-EPSCs for experiments illustrated in (E) (n = 11).

(G) A natural pattern of APs recorded in vivo from a CA3 pyramidal place cell was converted to current steps that were used to evoke APs in the postsynaptic CA3 pyramidal. The APs recorded in a CA3 pyramidal cell in the current clamp mode are shown in blue.

(H) Sample traces of Mf-EPSCs illustrating that DPE can be induced by a natural pattern of APs firing of CA3 pyramidal cells.

(I) Summary time course of normalized Mf-EPSCs for experiments illustrated in (G) (n = 9).

presynaptic boutons and focal AA uncaging, we observed that AA action mainly results in a direct inactivation of presynaptic Kv channels. This leads to the broadening of the presynaptic action potential (AP) and subsequent increase in transmitter release. Our results indicate that modulation of Kv channels by activity-dependent released lipids constitutes a powerful mechanism for tuning synaptic transmission, thus demonstrating the physiological significance of neuronal signaling mechanisms involving direct modulation of voltage-gated ion channels by lipids.

RESULTS

Retrograde Signaling at Mossy Fiber-CA3 Pyramidal Cell Synapses

Depolarization of neuronal membranes results in the calcium-dependent production of membrane-derived lipids, such as endocannabinoids mediating depolarization-induced suppression of inhibition (DSI) (Regehr et al., 2009; Wilson and Nicoll, 2002). We tested whether a similar protocol induced changes in synaptic transmission at Mf-CA3 synapses, which lack presynaptic CB$_1$Rs (Hofmann et al., 2008; Katona et al., 2006). The application of a depolarization step from −70 to −10 mV for 9 s in CA3 pyramidal cells induced a robust potentiation of

Mf-EPSCs (175% ± 13%, n = 12, p = 0.0005) (Figures 1A–1D), which peaked within 2–3 min and lasted up to 10–15 min. By analogy with DSI, we named this form of plasticity depolarization-induced potentiation of excitation (DPE). DPE varied in its magnitude with the duration of the depolarizing step (Figures S1A and S1B available online). The protocol could be repeated in the same cell (Figure S1C), and DPE magnitude was similar for two Mfs inputs independently stimulated and recorded in the same CA3 pyramidal cell (Figures S1D–S1F). However, DPE was not observed at associational/commissural (A/C) fiber synapses onto CA3 pyramidal cells (Figures S1G and S1H). Because a 9 s depolarizing step may not pertain to a physiological stimulus, we tested whether AP discharge in CA3 pyramidal cells also induced short-term potentiation of Mf-EPSCs. First, we applied a sequence of six bursts of five APs at 25 Hz in CA3 pyramidal cells at the frequency of theta oscillations (Buzsáki, 2005). This mild protocol induced transient potentiation of Mf-EPSCs (129% ± 9%, n = 11, p = 0.0137) (Figures 1E and 1F) to comparable levels as with a 9 s depolarization step with the same K$^+$-based intracellular solution (145% ± 16%, n = 11, p = 0.39). A similar potentiation could also be observed with bursts of spikes triggered by burst stimulation of Mf-CA3 synapses (eight stimulations at 25 Hz repeated six times at theta frequency; 136% ± 9%, n = 13) (Figures S1J–S1L). The facilitation induced by postsynaptic spikes in this protocol could be separated from the potent and short-lasting posttetanic potentiation
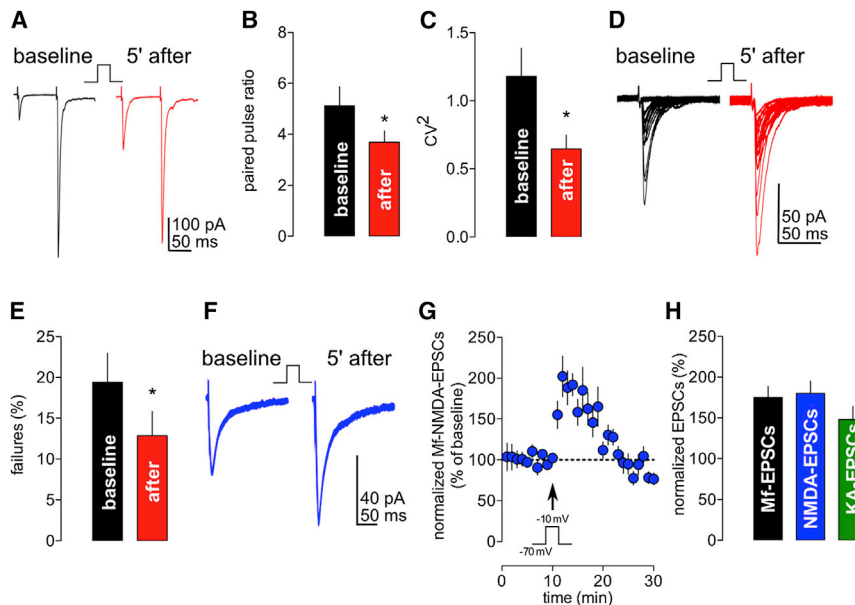
Figure 2. DPE Is Expressed Presynaptically

(A) Sample traces of paired pulse responses (100 ms interval) before and after DPE.

(B) Bar graph summarizing the values of PPR before and after DPE (n = 6, *p = 0.03, Wilcoxon match pairs test).

(C) Bar graph summarizing the change in CV^2 before and after DPE (n = 20, *p = 0.0018, Wilcoxon match pairs test). Values are presented as mean ± SEM of n experiments.

(D) Sample traces illustrating the marked reduction of synaptic failures (stimulation without detectable EPSCs) after DPE.

(E) Bar graph summarizing the significant reduction of synaptic failures after DPE (n = 14, *p = 0.021, Wilcoxon match pairs test).

(F) Sample traces of Mf-NMDA-EPSCs (recorded at −70 mV and in 0.3 mM Mg^{2+}) recorded before and after DPE induction.

(G) Summary time course for experiments illustrated in (C) (n = 8).

(H) DPE is similarly observed when recording Mf-EPSCs (essentially AMPA-EPSCs; n = 12) or isolated NMDA or Kainate-EPSCs (n = 8 and n = 6, respectively).

(Nicoll and Schmitz, 2005) with the use of 20 mM 1,2-bis(o-aminophenoxy)ethane-N,N,N',N'-tetraacetic acid (BAPTA) (94% ± 5%, n = 10, p = 0.0043, ctr versus BAPTA) in the patch pipette (see below and Figures S1J–S1L). Finally, we have used a natural pattern of spike discharge to induce DPE. A single sequence of APs (63 spikes over 18 s) recorded from a CA3 place cell in a freely moving rat entering in a place field (Isaac et al., 2009) was replayed into postsynaptic CA3 pyramidal cells with postsynaptic currents injection, and its effect was continuously recorded while evoking Mf-EPSCs at a frequency of 0.1 Hz (Figures 1G and 1H). This natural sequence of spiking activity enhanced the amplitude of Mf-EPSCs for several minutes (131% ± 10%, n = 9, p = 0.0391). These results indicate that physiologically relevant patterns of CA3 pyramidal cells firing can trigger DPE.

Next, we evaluated whether DPE was expressed pre- or postsynaptically. DPE was accompanied with a significant decrease in paired-pulsed facilitation (baseline, 5.1 ± 0.7; DPE, 3.7 ± 0.4; n = 6, p = 0.03), coefficient of variation (CV^2; baseline: 1.2 ± 0.2; DPE: 0.6 ± 0.1, n = 20, p = 0.0018), and failure rate (baseline: 19.4% ± 3.6%; DPE 12.9% ± 3.0%, n = 14, p = 0.021) (Figures 2A–2E), strongly suggesting a presynaptic mechanism. In addition, as expected for a presynaptic increase in glutamate release, isolated NMDA-EPSCs and Kainate-EPSCs were potentiated to similar extents after DPE (NMDA-EPSCs: 180% ± 15%, n = 8; Kainate-EPSCs: 148% ± 16%, n = 6, p = 0.52) (Figures 2F–2H). Finally, no potentiation was observed when replacing Mf simulation with focal UV uncaging of glutamate at the location of Mf-CA3 synapses on proximal dendrites (Figures S2A–S2D). Hence, DPE is induced postsynaptically and expressed presynaptically.

Next, we tested whether DPE, like DSI, was dependent on an increase in postsynaptic Ca^{2+}. Replacing 0.2 mM EGTA with 20 mM BAPTA in the patch pipette solution (EGTA: 179% ± 14%, n = 13; BAPTA: 89% ± 9%, n = 10, p = 0.0012) or blocking

L-type Ca^{2+} channels with nifedipine (10 μM; 87% ± 10%, n = 9, p = 0.0013) abolished DPE (Figures 3A–3C). Furthermore, we investigated the nature of the retrograde messenger involved in DPE. Conventional neurotransmitters that could potentially be released from the somato-dendritic compartment of CA3 pyramidal cells, including glutamate, GABA, or adenosine (Ludwig and Pittman, 2003), did not appear to be involved in DPE (Table S1). In keeping with this observation, the infusion of botulinum toxin C1 (BotoxC1; 0.5 μM) in the intracellular patch solution to block Ca^{2+}-dependent vesicular release from the somato-dendritic compartment of CA3 pyramidal cells did not affect DPE (solvent: 165% ± 23%, n = 5; BotoxC1: 191% ± 20%, n = 8, p = 0.621) (Figures 3D and 3E). In contrast, BotoxC1 was effective in reducing the amplitude of AMPA-EPSCs both at Schaffer collateral (Sc)-CA1 and Mf-CA3 synapses (Figures S3A–S3D; Table S1), most likely by blocking exocytosis (Lüscher et al., 1999). This suggests that DPE relies on a retrograde messenger that is released in a nonvesicular manner, such as gases (i.e., nitric oxide [NO]) or membrane-derived lipids (Regehr et al., 2009). Interestingly, although gases and membrane-derived lipids were shown to be capable of spreading their signal to neighboring neurons (Regehr et al., 2009), we found that DPE was restricted to the Mf afferences of the depolarized cell (DPE: 163% ± 20%; no DPE: 85 ± 4; n = 11) (Figures 3F–3H).

DPE Depends on Membrane-Derived Lipids

Blocking NO synthesis with L-NG-monomethyl arginine citrate or blocking NO-sensitive guanylyl cyclases with 1H-[1,2,4]oxadiazolo[4,3-a]quinoxalin-1-one did not affect DPE (n = 12, p = 0.653) (Figures S3E and S3F; Table S1). To test for an implication of membrane-derived lipids in DPE, we focused our attention on enzymes involved in the Ca^{2+}-dependent synthesis or in the degradation of the most common lipid messengers known, such as the endocannabinoids 2-AG (2-arachidonoylglycerol)
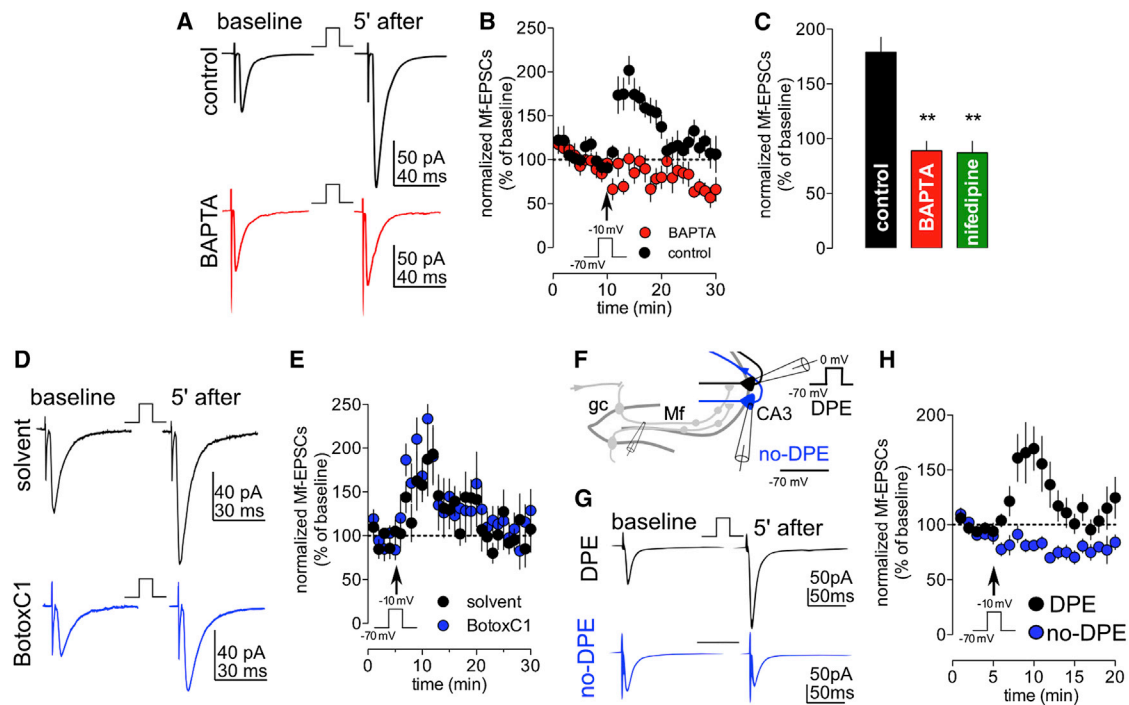
Figure 3. DPE Depends on Postsynaptic Calcium Rise and on a Nonvesicular Release Mechanism

(A–C) Sample traces, summary time course and bar illustrating that DPE is blocked by intracellular perfusion with BAPTA (10–20 mM) or bath application of the VGCC blocker nifedipine (10 μM; BAPTA, n = 10, **p = 0.0012; nifedipine, n = 9, **p = 0.0013, Kruskal-Wallis test).

(D and E) sample traces and summary time course showing that DPE is not blocked by inclusion of BotoxC1 (0.5 μM) in the patch pipette (solvent n = 5; BotoxC1 n = 8).

(F–H) DPE does not spread to neighboring neurons. CA3 pyramidal cells in organotypic slice cultures are highly packed, making this preparation ideal for investigating whether DPE can spread between two neighboring CA3 pyramidal cells.

(F) Two neighboring CA3 pyramidal cells were simultaneously patched, and only one received the depolarizing step.
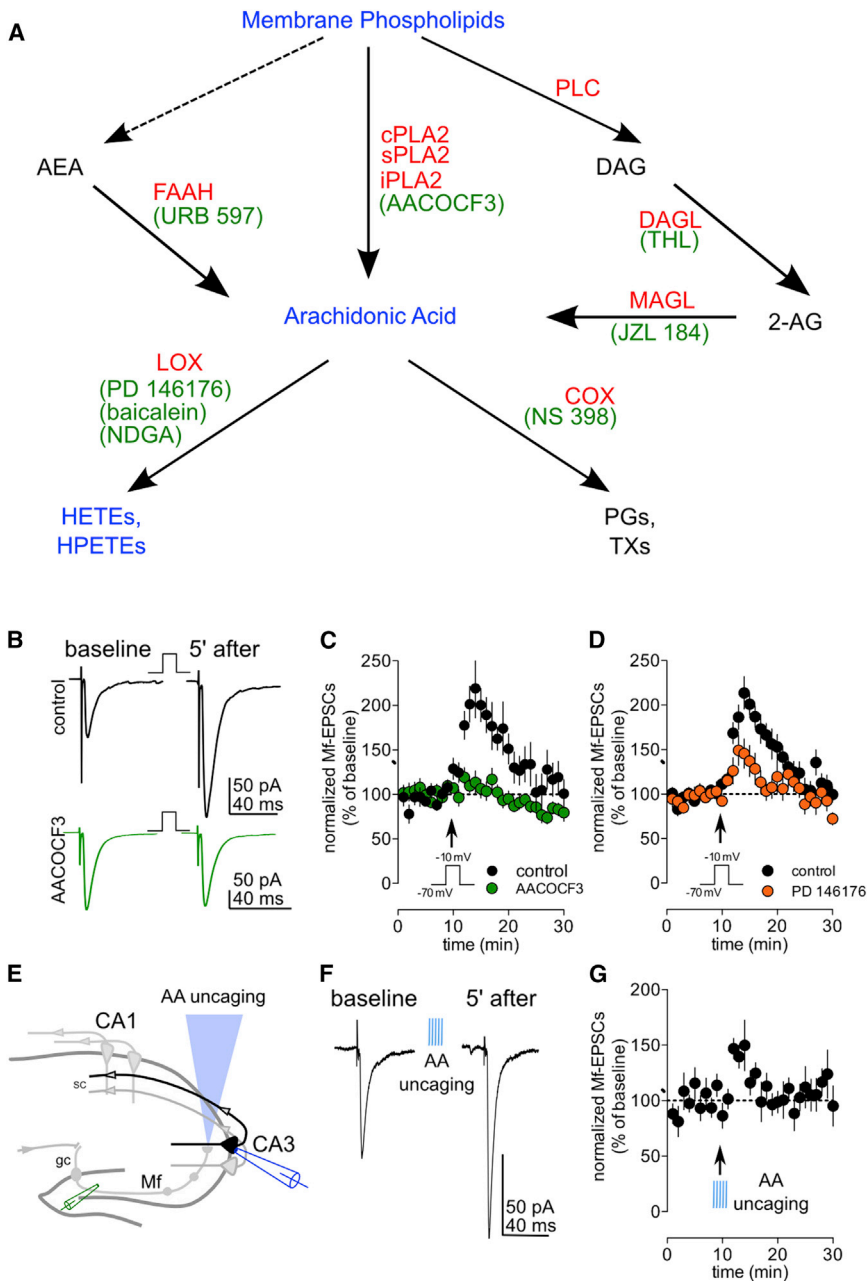
(G and H) Sample traces and time course illustrating that DPE is confined to the depolarized neuron (n = 11). Values are presented as mean ± SEM of n experiments.

and anandamide (Chevaleyre et al., 2006). DPE was not affected when perturbing the synthesis of 2-AG with the inhibitor of the diacylglycerol lipase, tetrahydrolipstatine (5 μM, n = 9, p = 0.841) (Figures 4A, S4A, and S4F; Table S1) nor when perturbing the degradation of anandamide with the inhibitor of fatty acid amide hydrolase, 3′-(aminocarbonyl)[1,1′-biphenyl]-3-yl)-cyclo-hexylcarbamate (1 μM, n = 15, p = 0.146) (Figures 4A, S4B, and S4F; Table S1). Furthermore, blocking degradation of 2-AG with a selective inhibitor of monoacylglycerol lipase, JZL 184 (10 μM), did not affect DPE (n = 16, p = 0.417) (Figures 4A, S4C, and S4F; Table S1). These experiments argue against a role for 2-AG or anandamide as retrograde messengers for DPE. In contrast, we found that cytoplasmic phospholipase A2 (cPLA2), a key enzyme responsible for the Ca^{2+}-dependent release of AA from phospholipids (Lambeau and Gelb, 2008) is critically involved in DPE. Indeed, inhibition of cPLA2 with arachidonyl trifluoromethyl ketone (AACOCF3; 10 to 20 μM) fully prevented DPE (ctr: 197% ± 17%, n = 13; AACOCF3: 110% ± 7%, n = 20, p = 0.0001) (Figures 4A–4C). PLA2 inhibition also prevented the enhancement of Mf-EPSCs induced by AP discharge evoked in CA3 pyramidal cells either with the natural firing protocol (ctr: 131% ± 10%, n = 9; AACOCF3: 90% ± 6%, n = 7, p = 0.0079) or through burst stimulation of Mf-CA3 synap-

ses (ctr: 136% ± 9%, n = 13; AACOCF3: 105% ± 8%, n = 12, p = 0.028) (Figure S1L). AA can be further metabolized by cyclo-oxygenases (COX), for example to prostaglandins, or by lipoxy-genases (LOX), to produce downstream products such as hydroxyperoxyeicosatetraenoic acids (HPETEs) or hydroxyei-cosatetraenoic acids (HETEs) (Figure 4A). The COX2 inhibitor N-(2-cyclohexyloxy-4-nitrophenyl) methanesulfonamide had no effect on DPE ruling out the participation of its downstream products (data not shown). In contrast, blocking LOX with PD 146176 (10 μM, 12- and 15-LOX inhibitor), baicalein (10 μM, 5- and 12-LOX inhibitor), or nordihydroguaiaretic acid (NDGA; 50 μM), a general LOX inhibitor, significantly reduced DPE (ctr: 191% ± 10%, n = 23; PD 146176: 137% ± 15%, n = 17, p = 0.0014; baicalein: 152% ± 9%, n = 13, p = 0.0297; NDGA: 114% ± 13%, n = 7, p = 0.0059) (Figures 4A, 4D, and S4D–S4F), suggesting the participation of downstream product of AA catabolism by LOX.

To test whether AA can itself increase synaptic transmission, we synthesized caged AA (see the Experimental Procedures). Focal photoactivation of 7-(diethylamino)-coumarin-4-yl-methyl arachidonate (caged AA, 10 μM; a concentration which is well within a physiologically relevant range) (Meves, 2008) onto CA3 pyramidal cell proximal dendrites induced transient potentiation

Figure 4. DPE Is Mediated by a Metabolite of cPLA2 and Can Be Mimicked by Exogenous Arachidonic Acid

(A) Signaling cascade for the metabolism of membrane phospholipids with the respective enzymes (red) and corresponding blockers used (green). AEA, anandamide; COX, cyclooxygenase; CYP, cytochrome P450; DAGL, DAG lipase; FAAH, fatty acid amide hydrolase; HETE, hydroxyeicosatetraenoic acid; HPETE, hydroperoxyeicosatetraenoic acid; LOX, lipoxygenase; MAGL, MAG lipase; NDGA, nordihydroguaiaretic acid; PG, prostaglandin; cPLA2, cytoplasmic phospholipase A2; PLC, phospholipase C.

(B) Sample traces illustrating the abrogation of DPE by incubating the slice (>30 min) with the PLA2 inhibitor AACOCF3 (10–20 μM).

(C) Summary time course for experiments illustrated in (B) (ctr, n = 13; AACOCF3, n = 20).

(D) DPE was reduced by slice incubation with the LOX inhibitor PD-146176 (10 μM; ctr, n = 23; PD-146176, n = 17).

(E) Caged AA (10 μM) was perfused in the slice for 10–15 min before flashing a UV light in the *stratum lucidum* near the recorded CA3 pyramidal cell.
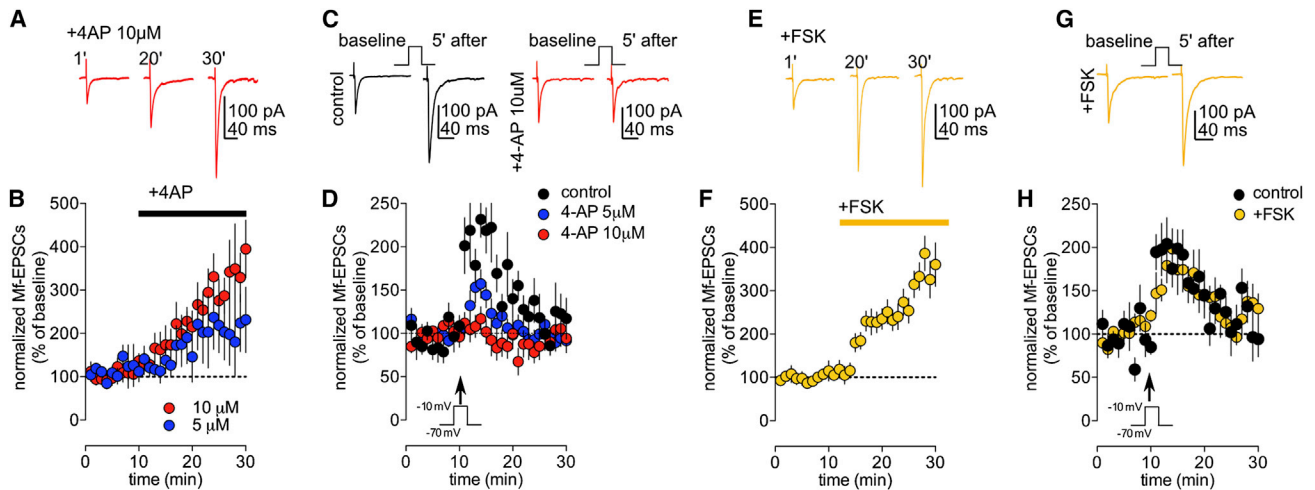
(F) Sample traces illustrating the transient potentiation of Mf-EPSCs induced by AA uncaging.

(G) Summary graph for experiments illustrated in (F) (n = 7). Values are presented as mean ± SEM of n experiments.

(capsazepine) (Gibson et al., 2008) or GPR55 (cannabidiol) (Ryberg et al., 2007) did not affect DPE (Figures S4I–S4K; Table S1). Protein kinase C (PKC) is another possible target of AA. It has been reported that AA and some of its derivatives can indirectly facilitate PKC activation (Schaechter and Benowitz, 1993). Similar to protein kinase A (PKA), PKC activation facilitates synaptic transmission at Mf-CA3 synapses. However, PKC or PKA activity was not required for DPE (Figures S4L–S4U; Table S1).

AA and some of its derivatives are also known to directly modulate voltage-gated ion channels (Fink et al., 1998). Interestingly, AA induces C-type inactivation of voltage-gated potassium channels (Kv) (Oliver et al., 2004). Cumulative inactivation or pharmacological blockade of presynaptic Kv channels induce a broadening of the AP waveform at Mf bouton (MfB) that results in increased glutamate release (Geiger and Jonas, 2000). To test whether presynaptic Kv channels could be the targets of AA released during DPE, we examined whether blocking Kv channels with low concentrations of 4-aminopyridine (4-AP; 5 or 10 μM) occluded DPE. At these concentrations, 4-AP considerably increased basal synaptic transmission at Mf-CA3 synapses (n = 7 and n = 6 for 4-AP 5 and 10 μM, respectively) (Figures 5A and 5B). Preincubation of the slices with 4-AP significantly

of Mf-EPSCs (145% ± 9%, n = 7, p = 0.0156), confirming that AA can indeed increase transmitter release at Mf-CA3 synapses (Figures 4E–4G).

DPE Occurs via 4-AP-Sensitive Potassium Channels

Next, we sought to identify a putative presynaptic target for AA (or a LOX product of AA). DPE was not affected by pharmacological inhibition of CB$_1$ or CB$_2$ receptors by SR141716A and AM 630, respectively (Figures S4G, S4H, and S4K; Table S1), consistent with the finding that DPE does not rely on the production of endocannabinoids. In addition, antagonists against known CNS lipid receptors such as TRPV1

Figure 5. DPE Occurs via 4-AP-Sensitive Potassium Channels

(A and B) Sample traces and time course illustrating the potentiating effect of 5 and 10 μM 4-AP on Mf-EPSCs (average at 25–30 min; 5 μM 4-AP, 207% ± 70%, n = 7; 10 μM 4-AP, 333% ± 34%, n = 6).

(C) Sample traces illustrating occlusion of DPE by preincubation of slices with 4-AP (10 μM).

(D) Summary of the experiments showing occlusion of DPE by 4-AP (ctr, n = 11; 4-AP 5 μM, n = 13; 4-AP 10 μM, n = 9).

(E and F) Potentiation of Mf-EPSCs by forskolin (10 μM; 344% ± 28%, n = 12).

(G and H) Sample traces and summary graph showing that DPE amplitude is not affected when Mf-EPSCs are previously potentiated by forskolin (10–20 μM; ctr, n = 6; forskolin, n = 12). DPE was induced 20–30 min after forskolin application when potentiation of Mf-CA3 synaptic transmission had reached a plateau. Values are presented as mean ± SEM of n experiments.

reduced DPE (ctr: 211% ± 15%, n = 11; 5 μM 4-AP: 145% ± 12%, n = 13, p = 0.0023; 10 μM 4-AP: 114% ± 7%, n = 9, p = 0.0005) (Figures 5C and 5D). The reduction in DPE magnitude did not simply result from a ceiling effect, given that forskolin (10 μM), a known potentiator of Mf-CA3 synapses via the activation of the PKA pathway, increased basal synaptic transmission (n = 12) (Figure 5E and 5F) but did not occlude DPE (ctr: 193% ± 18%, n = 6; forskolin: 193% ± 21%, n = 12, p = 0.4790) (Figures 5G and 5H). Similarly, DPE was not occluded by previously induced presynaptic LTP (Figure S5).
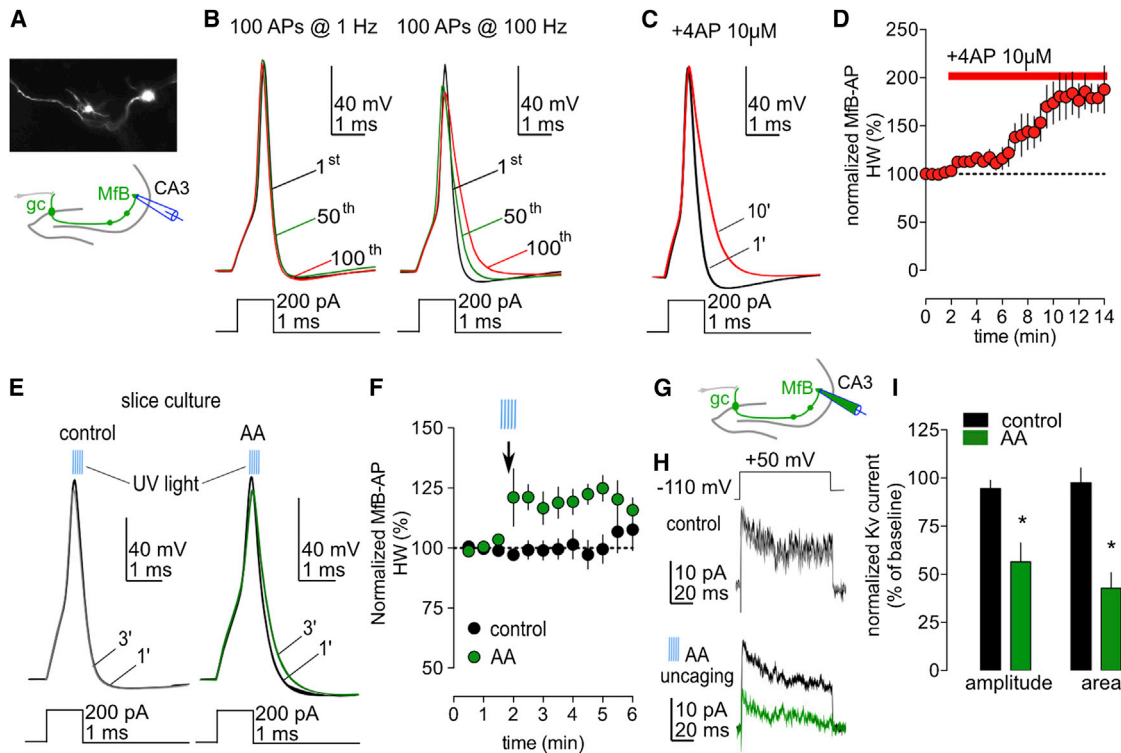
AA Induces the Broadening of Mf-Presynaptic Action Potentials

Thus, we reasoned that AA released from CA3 pyramidal cells during DPE may result in the broadening of MfB APs by the inactivation of 4-AP-sensitive presynaptic Kv channels. To test this hypothesis, we performed patch-clamp recordings from MfBs in organotypic cultures from Thy1-GFP mice (DPE was similarly observed in this preparation) (Figures 3F–3H), which significantly improved identification of MfBs (Figure 6A, S6A, and S6B) (Galimberti et al., 2006). APs triggered by current injection and recorded from MfBs in the current clamp mode displayed previously described property; i.e., marked frequency dependent broadening due to Kv channel inactivation (Figure 6B) (Geiger and Jonas, 2000). Moreover, in agreement with a previous study (Alle et al., 2011), low concentrations of 4-AP (10 μM), which considerably increased glutamate release at Mf synapses, also broadened APs (normalized AP half-width, 4-AP: 182% ± 15%, n = 5, p = 0.0313) (Figures 6C and 6D). We found that focal AA uncaging induced a rapid broadening of the presynaptic AP (normalized AP half-width values, at min 2–3: AA, 122% ± 6%,

n = 6; absolute AP half-width values: AA, baseline 0.55 ± 0.09 ms; after UV, at min 2–3: = 0.69 ± 0.09 ms; n = 6. p = 0.0313) (Figures 6E and 6F), which lasted several minutes. As a control, a similar UV flash given in the absence of the caged compound did not change AP half-width (normalized AP half-width values, at min 2–3: ctr, 99% ± 4%, n = 6; absolute AP half-width values: ctr, baseline = 0.54 ± 0.03 ms; after UV, at min 2–3: = 0.53 ± 0.03 ms, n = 6. Similar results were obtained in acute slices from P28-35 Thy1-GFP mice (Figures S6C and S6D). Thus, our functional and pharmacological data strongly suggest that AA may induce a broadening of APs via the inactivation of Kv channels in the MfB, which then results in an increased release of glutamate.

AA Inhibits Presynaptic Kv Currents

To further confirm that AA indeed modulates presynaptic Kv channels, we tested the effect of AA uncaging on isolated presynaptic Kv currents from MfBs. It has previously been shown that AA significantly reduces Kv currents in oriens-alveus interneurons (OA-I) in the CA1 region (Oliver et al., 2004). First, to validate our assay, we tested AA uncaging on Kv currents recorded from OA-I interneurons in the CA1 area in the cell-attached configuration (Figures S6E–S6G). We found that pharmacologically isolated Kv currents recorded from the soma of OA-I interneurons were potently inhibited by AA uncaging (normalized amplitude, p = 0.0469; normalized area, p = 0.0156) (Figures S6F and S6G). Next, we tested the effect of AA uncaging on pharmacologically isolated Kv currents recorded from MfBs in the cell-attached configuration (Figure 6G). Kv currents recorded from MfBs were inhibited by AA uncaging (normalized amplitude, ctr: 94% ± 4%, n = 7; AA uncaging: 56% ± 9%, n = 7, p = 0.0156; normalized area, ctr: 97% ± 7%, n = 7; AA uncaging: 42% ± 8%,

Figure 6. AA Induces Mf-Presynaptic Action Potential Broadening by Inactivation of Presynaptic Kv Channels

(A) Hippocampal organotypic slices were prepared from Thy1-GFP mice to facilitate the visualization of MfBs.

(B) APs evoked by a 1 or 100 Hz train of brief current pulses (200 pA, 1 ms). Black, 1st AP; green, 50th AP; red, 100th AP. Traces were aligned to the onset of the current pulse. Note that AP broadening during repetitive stimulation (1st versus 100th), which is characteristic of MfBs and is mediated by activity-dependent inactivation of presynaptic Kv channels.

(C and D) Sample traces (average of 15–20 sweeps) illustrating that the AP half-width (HW) increases with 4-AP (10 μM; n = 5).

(E) Sample traces (average of three to five sweeps) illustrating that the AP HW increases after AA uncaging. No significant changes were observed in control experiments (UV light applied in the absence of caged AA).

(F) Time course for AA uncaging experiments illustrated in (F) (ctr, n = 6; AA, n = 6). Values are presented as mean ± SEM of n experiments.

(G and H) Sample traces (average of five to six sweeps) illustrating the inhibitory effect of AA uncaging on the amplitude and area of the Kv currents recorded from MfB in the cell-attached configuration. Caged AA (10 μM) was dissolved in the patch pipette solution. A 500 ms prepulse to −110 mV was applied. No change in the currents over time was observed in control experiments (no UV light applied).

(I) Summary graph of the effect of AA uncaging as illustrated in (F) (ctr, n = 7; AA, n = 7; *p = 0.0156, Wilcoxon match pairs test).

n = 7, p = 0.0156) (Figures 6E and 6F). In an attempt to further characterize the mechanism by which AA inhibited Kv currents at MfBs, we have performed outside-out patch-clamp recordings from MfBs in acute slices. We found that AA shifted the voltage dependence of steady-state inactivation of pharmacological isolated Kv currents toward more negative values (Figures S6H and S6I) but did not affect the voltage dependence of activation of Kv currents from the same patches. These results show that Kv channels present at MfBs are highly sensitive to AA. Hence, our data strongly suggest that DPE results from a Ca^{2+}-dependent postsynaptic release of AA (or one of its derivatives) acting on presynaptic Kv channels in order to induce a broadening of APs, which, in turn, results in an increase of glutamate release (Figure 9). We thus report a form of short-term synaptic plasticity in the CNS resulting from the direct modulation of voltage-gated channels by endogenously released lipids.

Next, we aimed to directly investigate whether endogenous AA released from postsynaptic CA3 pyramidal cells could modu-

late the duration of presynaptic APs in MfBs. We have previously shown that burst stimulation of Mf-CA3 synapses induced the firing of CA3 pyramidal cells, which is sufficient to induce DPE (Figures S1J–S1L). Thus, we have monitored presynaptic AP waveform with patch-clamp recordings while inducing DPE with this protocol. We have triggered bursts of APs by direct current injection in the MfB to induce glutamate release and drive the connected postsynaptic CA3 pyramidal cell to spike and, ultimately, induce DPE (Figure 7). Bursts of action APs in the MfB lead to prolonged broadening of presynaptic APs, consistent with an inactivation of presynaptic Kv channels. This broadening displayed a slow onset similar to the time course of DPE (normalized AP half-width values at min 5–6 [3–4 min after the theta burst]: ctr, 127% ± 8%, n = 11; absolute AP half-width values: ctr, baseline = 0.53 ± 0.03 ms; after theta burst, at min 5–6 = 0.65 ± 0.03 ms, n = 11. p = 0.0049) (Figures 7B–7D). We performed two control experiments in order to verify that presynaptic AP broadening is mediated by postsynaptic AA release in
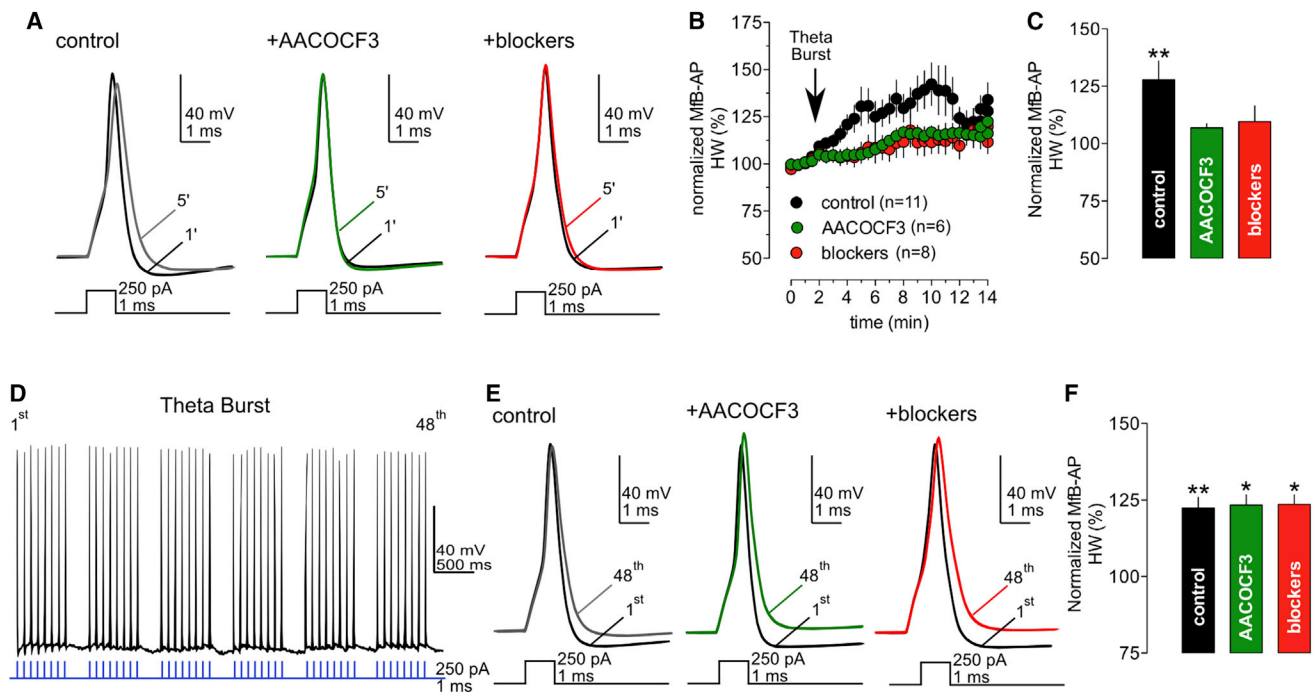
Figure 7. Theta Burst Firing in MfBs Induces AP Broadening, which Depends on PLA2 Activity and Activation of Glutamate Receptors in CA3 Pyramidal Cell

(A) Sample traces (average of three sweeps), illustrating that, in the control condition, the AP half-width is increased 3 min after the burst of APs (delivered at 2 min) in the MfB. No change in the AP duration was observed in the presence of the PLA2 inhibitor (AACOCF3, 20 μM) or a cocktail of glutamate receptor blockers (NBQX, AP5, mGluR1, and mGluR5).

(B) Time course for MfB burst experiments illustrated in (B) (ctr, n = 11; AACOCF3, n = 6; blockers, n = 8). Values are presented as mean ± SEM of n experiments.

(C) Bar graph summarizing the changes in AP half-width at 5–6 min, 3 min after the theta burst in the MfB.

(D) Sample trace illustrating the brief burst of APs triggered by burst injection of currents (eight APs at 25 Hz, repeated six times at theta frequency, 140 ms interval).

(E) Sample traces illustrating that the broadening of the AP (comparing the 1st versus the 48th AP of the burst) does not differ among different experimental conditions.

(F) Bar graph summarizing the changes AP HW (1st versus the 48th) during the burst in the MfB (ctr, n = 11; AACOCF3, n = 6; blockers, n = 8). Values are presented as mean ± SEM of n experiments (*p = 0.0156, **p = 0.002 - 0.0049, Wilcoxon match pairs test).

these conditions. First, we showed that AP broadening was inhibited by the PLA2 inhibitor AAFCOF3 (normalized AP half-width values at min 5–6 [3–4 min after the theta burst]: AACOCF3, 107% ± 2%, n = 6; absolute AP half-width values: AACOCF3, baseline = 0.47 ± 0.04 ms; after theta burst, at min 5 to 6 = 0.49 ± 0.04 ms, n = 6) (Figures 7B–7D). Second, we showed that the broadening of presynaptic APs requires synaptic activation of glutamate receptors which drive postsynaptic firing. In the presence of a cocktail of ionotropic and metabotropic glutamate receptor antagonists, no broadening of presynaptic APs was observed after burst stimulation (normalized AP half-width values at min 5 to 6 [3 to 4 min after the theta burst]: blockers, 109% ± 7%, n = 8; absolute AP half-width values: blockers, baseline = 0.60 ± 0.03 ms; after theta burst, at min 5 to 6 = 0.61 ± 0.03 ms, n = 8) (Figures 7B–7D). In the absence of burst stimulation, the duration of presynaptic APs over time did not differ between control conditions and during pharmacological treatments (data not shown). These results provide clear evidence that burst stimulation of presynaptic Mf terminals results in prolonged presynaptic AP broadening mediated by lipid

messengers produced via increase in postsynaptic PLA2 activity. Importantly, the pharmacological treatments did not affect the capability of MfBs to undergo short-term use-dependent broadening during a theta burst stimulation per se (normalized AP half-width values 48th versus 1st: ctr, 122% ± 3%, n = 8; AACOCF3, 123% ± 3%, n = 6; blockers, 123% ± 3%, n = 8; absolute AP half-width values: ctr, 1st = 0.59 ± 0.03 ms; 48th = 0.72 ± 0.04 ms, n = 11, p = 0.002; AACOCF3, 1st = 0.46 ± 0.04 ms; 48th = 0.56 ± 0.05 ms, n = 6, p = 0.0156; blockers, 1st = 0.64 ± 0.03 ms; 48th = 0.79 ± 0.05 ms, n = 8, p = 0.0156) (Figures 7E–7G) (Geiger and Jonas, 2000).

DPE Facilitates LTP Induction at Mf-CA3 Synapses

Although there is a strong agreement that Mf-LTP is expressed presynaptically at Mf-CA3 synapses, the participation of the postsynaptic neuron in its induction has been a matter of debate (Mellor and Nicoll, 2001; Nicoll and Schmitz, 2005; Yeckel et al., 1999). Thus, we asked whether DPE could modulate presynaptic Mf-LTP; i.e., whether the transient increase of synaptic transmission induced by DPE could facilitate LTP induction. A single
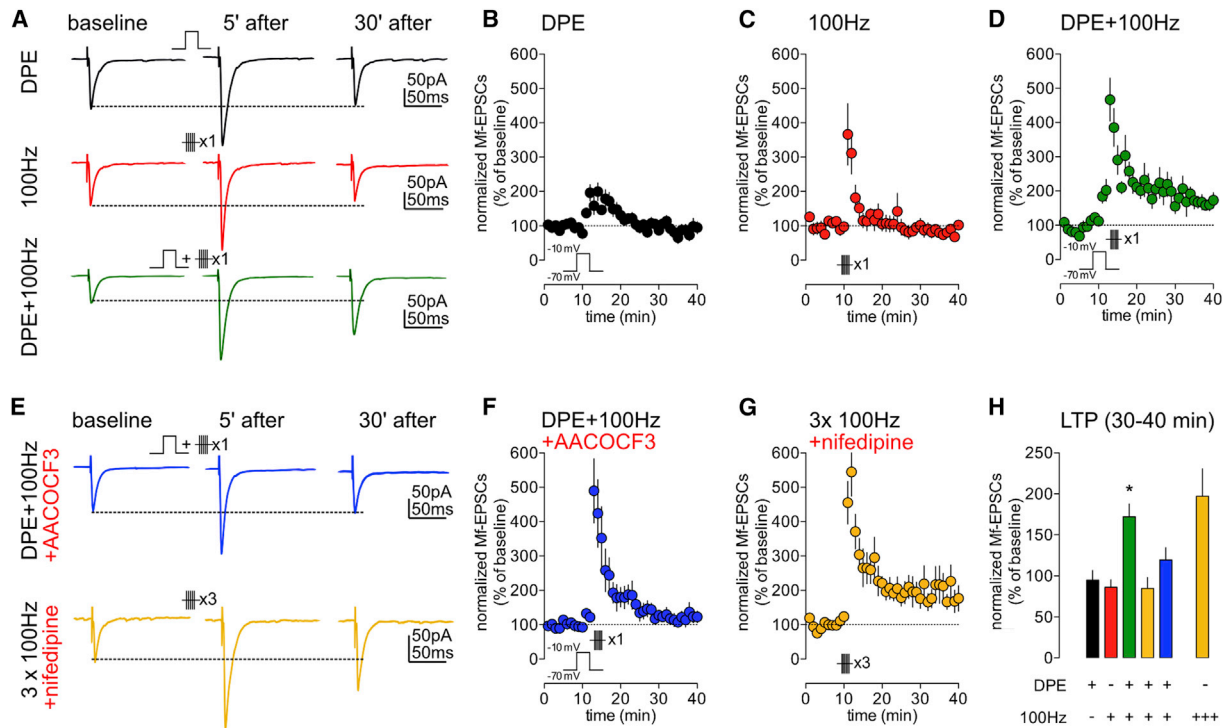
Figure 8. DPE Lowers the Threshold for Long-Term Potentiation of Mf-EPSCs

(A) Sample traces showing that both DPE and a single HFS train (100 stimuli at 100 Hz) fail to induce long-term potentiation of Mf-EPSCs (Mf-LTP). DPE followed 2 min later by a single HFS train induces Mf-LTP.

(B–D) Summary of the data presented in (A) (100 Hz, n = 6; DPE, n = 9; DPE + 1 HFS, n = 9).

(E) Sample traces illustrating that Mf-LTP observed in (D) is abrogated with AACOCF3 (10 μM). The bottom panel shows that, conversely, presynaptic Mf-LTP can be induced by three HFS even in the presence of nifedipine, indicating that postsynaptic L-type calcium channels are not absolutely required for Mf-LTP.

(F and G) Summary of the experiments presented in (E) (DPE + 1 HFS in the presence of AACOCF3, n = 7; three HFS, n = 5).

(H) Bar graph summarizing the results presented in (B), (C), (D), (F), and (G). Values are presented as mean ± SEM of n experiments (*p = 0.0139, Kruskal-Wallis test).

high-frequency stimulation (HFS) train (100 stimuli at 100 Hz) or the 9 s DPE protocol did not induce any long-lasting potentiation of Mf-EPSCs (35–40 min after the protocol; HFS: 86% ± 9%, n = 6; DPE: 94% ± 11%, n = 9) (Figures 8A–8C and 8H). However, when this single HFS train was applied 2 min after the induction of DPE (at the time in which potentiation is maximal), a long-lasting potentiation of Mf-EPSCs was observed (DPE + 1 HFS: 172% ± 16%, n = 9, p = 0.0139) (Figures 8A, 8D, and 8H). Blocking DPE induction with nifedipine (10 μM) or AACOCF3 (10 to 20 μM) abolished LTP induced by a single train and the 9 s DPE protocol (DPE + 1 HFS: nifedipine, 84% ± 13%, n = 7; AACOCF3, 119% ± 14%, n = 8) (Figures 8E, 8F, and 8H), whereas the conventional presynaptic LTP induced by three HFS trains was not blocked by nifedipine (10 μM; 3 HFS: 215% ± 60%, n = 5) (Figures 8E, 8G, and 8H). Our results confirm numerous studies that have indicated that there is no strict requirement for a rise of Ca²⁺ or depolarization of the postsynaptic CA3 pyramidal cell for inducing presynaptic Mf-LTP (Mellor and Nicoll, 2001). However, we show that a postsynaptic rise of Ca²⁺ in postsynaptic CA3 pyramidal cells, by triggering DPE, facilitates the induction of LTP. Thus, our data shed light on the discrepancies in the literature on the participation of CA3 pyramidal cells in Mf-LTP (Yeckel et al., 1999). The most likely explanation

for a change in threshold for presynaptic LTP with DPE lies in the increased activation of voltage-dependent Ca²⁺ channels (Breustedt et al., 2003; Dietrich et al., 2003) during the tetanus, resulting in higher Ca²⁺ influx and facilitation of the activation of Ca²⁺-dependent adenylyl cyclases AC1 and AC8 (Figure 9) (Villacres et al., 1998; Wang et al., 2003).

DISCUSSION

Membrane-derived lipids are important signaling molecules used by neurons to modulate synaptic transmission. In the CNS, neuronal depolarization is known to increase the production of lipid messengers, which either act on the neuron where they are produced or diffuse away and modulate presynaptic inputs (Regehr et al., 2009; Wilson and Nicoll, 2002). Almost all presynaptically acting lipid messengers reported so far induce a decrease in neurotransmitter release, mainly by activating CB₁ or TRPV1 receptors (Regehr et al., 2009). Apart from their action through specific receptors, lipids are also known to directly act on voltage-gated ion channels in order to modulate their function (Boland and Drzewiecki, 2008). However, an endogenous mechanism employing such a direct modulation of voltage-gated ion channels by membrane-derived lipids has
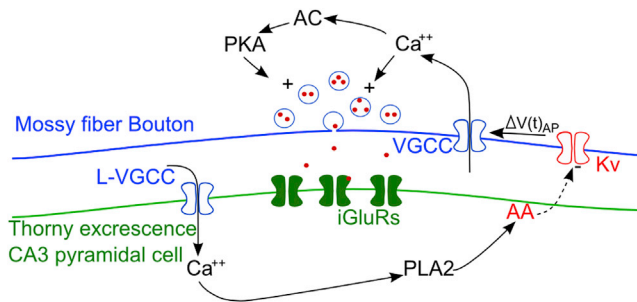
Figure 9. Working Model for the Mechanism of DPE

Depolarization of a CA3 pyramidal cell triggers voltage-dependent Ca²⁺ channels activation. Elevation of intracellular Ca²⁺ concentration activates cPLA2, leading to the release of AA. AA inhibits presynaptic 4-AP-sensitive Kv channels, inducing a broadening of the AP in the presynaptic Mf bouton, and subsequent increased release of glutamate. This retrograde signaling mechanism decreases the threshold for triggering presynaptic LTP of Mf-CA3 synapses.

not yet been reported. Recently, it was shown that 2-AG directly modulates GABA$_A$ receptors, and this modulation has a potential impact on mouse behavior (Sigel et al., 2011), supporting the idea that membrane-derived lipids can, in principle, modulate neuronal signaling not only through membrane receptors but also through direct modulation of ion channels.

Here, we identify a retrograde signaling mechanism by which endogenously released membrane-derived lipids potentiate synaptic transmission through the inhibition of presynaptic Kv channels. Exogenously applied AA appears to regulate synaptic transmission by a variety of mechanisms (Darios et al., 2007; Meves, 2008; Piomelli et al., 1987; Williams et al., 1989), although a role for AA at vertebrate CNS synapses has been challenged (O'Dell et al., 1991). The present study demonstrates that AA (or one of its metabolites) is released in an activity-dependent manner at Mf-CA3 synapses and acts as a retrograde messenger in order to facilitate synaptic transmission. Moreover, we show that 4-AP-sensitive Kv channels represent a target for presynaptic modulation of neurotransmitter release by a lipid-mediated retrograde mechanism.

Mechanisms and Properties of DPE

Here, we propose that DPE results from the Ca²⁺-dependent release of AA from postsynaptic CA3 pyramidal cells, which then acts as a retrograde messenger in order to broaden presynaptic APs, subsequently potentiating synaptic transmission. Methodologically, lipid uncaging offers the possibility for acute and local manipulation of lipid second messenger concentration (Nadler et al., 2013). This approach allows rapid changes in the concentration of a lipid in a focal neuronal domain in a slice preparation, which is difficult to achieve with bath application of AA. Focal uncaging of AA induced a transient potentiation of Mf-CA3 synapses, a broadening of the presynaptic AP, and an inactivation of Kv channels recorded in patches from MfBs. The AA-induced broadening of the AP was fast in onset and lasted for several minutes, with a time course comparable to the effect of uncaged AA on Mf-EPSCs. The slow decay of AA broadening may be partly due to the off kinetics of AA from Kv

channels and/or to the slow washout of AA. It has been reported that the effects of AA on Kv channels in heterologous expression systems and in the slice preparation could only be reverted after the addition of BSA (Villarroel and Schwarz, 1996). Moreover, as to the duration of DPE itself, the enzymatic machinery involved in the release of AA may, in addition, display slow kinetics. Interestingly, other well-characterized forms of lipid-mediated short term plasticity, namely DSI and DSE, display faster decay kinetics on the order of tens of seconds (Regehr et al., 2009). Whether these differences are due to the enzymatic processes (synthesis and clearance), the nature of the retrograde messenger, or the presynaptic effector is unknown. We show that presynaptic Kv channels sensitive to low concentrations of 4-AP are the likely targets of AA in DPE. Kv channels are known to be highly sensitive to several lipids, especially AA (Meves, 2008). We propose that AA uncaging induces inactivation of Kv channels recorded in patches from MfBs by shifting the voltage dependence of steady-state inactivation toward more negative values. This is well in line with observations of the effects of AA on somatic Kv channels recorded from CA1 pyramidal cells (Angelova and Müller, 2006; 2009).

In control conditions, presynaptic APs at Mf-CA3 synapses are short during low-frequency stimulation but are prolonged up to 3-fold during HFS (100 Hz) as a consequence of cumulative Kv channel inactivation (Geiger and Jonas, 2000). High-frequency-mediated AP broadening only requires discharge of presynaptic APs (Geiger and Jonas, 2000) but not the activation of PLA2. In contrast, DPE depends on the depolarization or spiking activity of the postsynaptic neuron but not on the presynaptic AP discharge. In addition, frequency-dependent broadening of presynaptic APs lasts only seconds (Geiger and Jonas, 2000) as opposed to several minutes for DPE. Hence, DPE and the short-lived broadening of APs by HFS represent two different modes of regulation of presynaptic APs with distinct mechanisms and kinetics that may coexist at the same synapse. It may be possible that, at a high frequency of presynaptic APs, AA-mediated inhibition will be less effective given that Kv channels are already inactivated because of their intrinsic gating properties. In all DPE experiments, presynaptic stimulation was kept at 0.1 Hz, where there is no activity-dependent inactivation of presynaptic Kv channels.

AA induces the broadening of presynaptic APs by about 25%. Several previous studies point out that the relationship between presynaptic AP width and synaptic strength is not linear. For instance, at parallel fiber Purkinje cell synapses, a 23% increase in spike width lead to a 25% increase in total calcium and to a doubling of synaptic strength (Sabatini and Regehr, 1997). At Mf-CA3 synapses, a prolongation of the presynaptic AP by 33%, increased the Ca²⁺ charge by 27%, which, in turn, increased the EPSC peak amplitude by 77% (Geiger and Jonas, 2000). Hence, we hypothesize that the AA-induced broadening of the AP leads to enhanced synaptic transmission by increasing the AP-driven Ca²⁺ influx in presynaptic terminals. The changes in Pr after Mf-LTP most likely involve changes in the release machinery (Nicoll and Schmitz, 2005). However, Mf-LTP is not thought to be expressed as a change in AP-driven Ca²⁺ influx (Kamiya et al., 2002). Accordingly, potentiation induced by Mf-LTP did not occlude DPE. Therefore, the

potentiation induced by Mf-LTP and DPE are most likely parallel mechanisms.

Is DPE a Widespread Mechanism?

cPLA2 is expressed in most regions of the brain and predominantly in neurons (Kishimoto et al., 1999), suggesting that DPE and modulation of transmitter release following Ca^{2+}-dependent cPLA2 activation may be a general phenomenon observed at other central synapses. We observed a robust potentiation of synaptic transmission through DPE at Mf-CA3 synapses but not at A/C-CA3 glutamatergic synapses. At least three reasons may explain this difference. First, the extent of DPE and the conditions of induction possibly vary depending on the sensitivity or type of presynaptic Kv channels or other ion channels, the local density of voltage-gated Ca^{2+} channels, or other sources of Ca^{2+}, such as the activity of mGluRs. Second, the particular architecture of Mf synapses, with a large presynaptic terminal enwrapping the complex and large postsynaptic thorny excrescences may also favor production and accumulation of membrane-derived lipid messengers. Third, Mf-CA3 synapses lack presynaptic CB_1Rs, which mediate short-term inhibition of glutamate release at other synapses. An interesting hypothesis would be that, at certain synapses, the inhibition of synaptic transmission through activity-dependent release of endocannabinoids and activation of CB_1Rs counterbalances the potentiation induced by AA-mediated inhibition of presynaptic Kv channels. The balance between CB_1-dependent inhibition and DPE could be fine-tuned by CB_1Rs expression levels at presynaptic sites.

We have directly tested this hypothesis at Sc-CA1 synapses which express DSE (Depolarization-induced Suppression of Excitation), a short-lasting inhibition of Sc-CA1 synaptic transmission dependent on endocannabinoid signaling and activation of CB_1Rs (Ohno-Shosaku et al., 2002). We showed that a DPE-like phenomenon can be observed at Sc-CA1 synapses in conditions where endocannabinoid signaling was abrogated by blocking presynaptic CB_1Rs (Figure S7). This transient potentiation of Sc-CA1 synaptic transmission was blocked by AACOCF3, the cPLA2 antagonist. In fact, it was previously shown that inhibiting CB_1Rs in dorsal raphe neurons not only blocked DSE but unexpectedly elicited a transient potentiation of EPSC amplitude similar in magnitude and timing to DPE (Haj-Dahmane and Shen, 2009). An additional example is given by the analysis of mice deficient for diacylglycerol lipase (DGL-α) which produces 2-arachidonoylglycerol (2-AG) involved in DSE at central synapses (Tanimura et al., 2010). Interestingly, in these mice, the abolition of DSE at parallel fiber to Purkinje cell synapses unravelled a transient potentiation of synaptic transmission with kinetic and amplitude similar to what we are now reporting at Sc-CA1 synapses (Tanimura et al., 2010). Hence, we can conclude that DPE could be more widespread in the brain, and in particular be prevalent at synapses which do not express CB_1Rs.

Physiological Relevance of DPE

DPE is not only induced by a steady-state depolarization of the postsynaptic neuron but also by protocols that pertain to physiological hippocampal activity. Indeed, DPE can be triggered by a sequence of a few short bursts of postsynaptic APs repeated at the frequency of theta oscillations, which are thought to facilitate the formation of maps and episodic/semantic memories (Buzsáki, 2005). Moreover, this transient potentiation is observed with a natural sequence of AP firing reproducing the spiking activity of a CA3 place cell of a rat exploring its environment (Isaac et al., 2009). Hence, DPE, which is expressed as a change in presynaptic properties, can be induced by the sole spiking activity of postsynaptic CA3 pyramidal cells but does not directly require synaptic activity. Nonetheless, bursts of spikes triggered by synaptic inputs (i.e., Mf-CA3 inputs) are also efficient in triggering DPE. However, in this case, DPE coexists with purely presynaptic forms of short-term facilitation that display in generally shorter time courses (Nicoll and Schmitz, 2005). Although DPE induction does not depend on presynaptic AP firing, we do not exclude that it could be modulated by incoming synaptic activity leading, for instance, to the activation of postsynaptic mGluRs and Ca^{2+} release from internal stores.

As a direct consequence of the fact that DPE can be induced by postsynaptic spiking activity, it will affect all Mf-CA3 synapses in a single CA3 pyramidal cell as opposed to other forms of short-term plasticity that are synapse specific. Concomitant to the fact that DPE does not spread to neighboring CA3 pyramidal cells, this process favors the emergence of an active CA3 pyramidal within the local network. By transiently facilitating synaptic transmission, DPE primes presynaptic long-term plasticity at all Mf synaptic inputs to a single CA3 pyramidal cell. This will most likely occur after a period of high spiking activity, such as when an animal explores its environment (Buzsáki, 2005). The priming event represented by DPE most likely enhances the capacity of local CA3 circuits to rapidly encode a novel context by facilitating long-term synaptic plasticity between dentate gyrus and CA3 pyramidal cells. Hence, the control of voltage-gated ion channels by activity-dependent release of membrane-derived lipids provides a mechanism for the dynamic regulation of neural circuits.

EXPERIMENTAL PROCEDURES

All the animal were used according to the guidelines of the University of Bordeaux/CNRS Animal Care and Use Committee.

Electrophysiology

Parasagittal hippocampal slices (320 μm) were obtained from 18- to 25-day-old C57Bl/6 mice. Slices were transferred to a recording chamber in which they were continuously superfused with an oxygenated extracellular medium (95% O_2 and 5% CO_2) containing 125 mM NaCl, 2.5 mM KCl, 2.3 mM $CaCl_2$, 1.3 mM $MgCl_2$, 1.25 mM NaH_2PO_4, 26 mM $NaHCO_3$, and 20 mM glucose (pH 7.4). Whole-cell recordings were made at ~32°C from CA3 pyramidal cells under infrared differential interference contrast imaging with borosilicate glass capillaries, which had resistances between 4–8 MΩ. For voltage-clamp recordings from CA3 pyramidal cells, the patch electrodes were filled with a solution containing 140 mM $CsCH_3SO_3$, 2 mM $MgCl_2$, 4 mM NaCl, 5 mM phospho-creatine, 2 mM Na_2ATP, 0.2 mM EGTA, 10 mM HEPES, and 0.33 mM GTP (pH 7.3) adjusted with CsOH. DPE was still observed when $CsCH_3SO_3$ was replaced by CsCl or KCl or by the larger cation ($NMDG^+$). DPE was not induced when QX314 (5 mM) was added to the intracellular solution (data not shown): QX314, largely used as Na^+ channel blocker, also blocks voltage-gated calcium channels (VGCC) and interferes with intracellular signaling (Talbot and Sayer, 1996). For current clamp recordings of CA3 pyramidal cells, the intracellular solution contained 140 mM KCH_3SO_3,

10 mM HEPES, 0.2 mM EGTA, 4 mM MgATP, 0.3 mM GTP, and 15 mM phosphocreatine (pH adjusted to 7.3 with KOH). No liquid-junction potential correction was used. Bicuculline (10 μM) was present in the superfusate of all experiments. A patch pipette (open tip resistance ∼5 MΩ [about 1 μm tip diameter]) was placed in the dentate gyrus to stimulate Mfs or in the *stratum radiatum* of the CA3 area to stimulate A/C fibers. Mf synaptic currents were identified according to the following criteria: robust low-frequency facilitation, low release probability at 0.1 Hz, rapid rise times of individual EPSCs (∼1 ms), and EPSC decays free of secondary peaks that may indicate the presence of polysynaptic contamination. Details for the electrophysiological procedures, including patch-clamp recordings of presynaptic boutons, are provided in the Supplemental Information.

Caged AA Synthesis and Uncaging

Caged AA was synthesized by esterification of AA with diethylamino-4-methylenhydroxycoumarin in the presence of carbodiimide and dimethylamino pyridine in 59% yield after purification by liquid chromatography (for synthetic details, see below). The hydroxycoumarin was prepared according to published procedures (Hagen et al., 2003; Meves, 2008).

A fresh aliquot of caged AA was used for each experiment and was dissolved in extracellular medium. The slices were perfused with extracellular medium containing caged AA for at least 10–15 min before starting the experiments in order to ensure homogenous penetration of the caged compound in the slice. During the application of caged AA, a total amount of 10 ml of extracellular solution containing the caged compound was continuously recirculated and oxygenated. AA was locally uncaged in the *stratum lucidum* of the patched CA3 pyramidal cell or the patched MfB by an UV flash photolysis (Xenon flash lamp, Rapp OptoElectronic). For cell-attached recordings, 10 μM caged AA was dissolved directly in the patch-pipette solution. Synthetic details are provided in the Supplemental Information.

Statistics

Values are presented as mean ± SEM of n experiments. For statistical analysis, nonparametric test were used. A Mann-Whitney test was used for two groups' comparison, and Kruskal-Wallis test followed by a Dunn's multiple comparison test for comparison between more than two groups. Within-cell comparisons were made with Wilcoxon match pairs test in raw nonnormalized values between baseline values and after values obtained after applying the desired protocol. Statistical differences were considered as significant at p < 0.05. Statistical analysis was performed with GraphPad Prism software.

All drugs were obtained from Tocris Cookson, Sigma-Aldrich, or Ascent Scientific. BotoxC1 was produced as in Vaidyanathan et al. (1999). The effects of pharmacological manipulations were always compared to interleaved control experiments.

SUPPLEMENTAL INFORMATION

Supplemental Information contains Supplemental Experimental Procedures, seven figures, and one table and can be found with this article online at http://dx.doi.org/10.1016/j.neuron.2013.12.028.

AUTHOR CONTRIBUTIONS

ACKNOWLEDGMENTS

REFERENCES

Alle, H., Kubota, H., and Geiger, J.R. (2011). Sparse but highly efficient Kv3 outpace BKCa channels in action potential repolarization at hippocampal mossy fiber boutons. J. Neurosci. *31*, 8001–8012.

Angelova, P., and Müller, W. (2006). Oxidative modulation of the transient potassium current IA by intracellular arachidonic acid in rat CA1 pyramidal neurons. Eur. J. Neurosci. *23*, 2375–2384.

Angelova, P.R., and Müller, W.S. (2009). Arachidonic acid potently inhibits both postsynaptic-type Kv4.2 and presynaptic-type Kv1.4 IA potassium channels. Eur. J. Neurosci. *29*, 1943–1950.

Besana, A., Robinson, R.B., and Feinmark, S.J. (2005). Lipids and two-pore domain K+ channels in excitable cells. Prostaglandins Other Lipid Mediat. *77*, 103–110.

Boland, L.M., and Drzewiecki, M.M. (2008). Polyunsaturated fatty acid modulation of voltage-gated ion channels. Cell Biochem. Biophys. *52*, 59–84.

Breustedt, J., Vogt, K.E., Miller, R.J., Nicoll, R.A., and Schmitz, D. (2003). Alpha1E-containing Ca2+ channels are involved in synaptic plasticity. Proc. Natl. Acad. Sci. USA *100*, 12450–12455.

Buzsáki, G. (2005). Theta rhythm of navigation: link between path integration and landmark navigation, episodic and semantic memory. Hippocampus *15*, 827–840.

Chevaleyre, V., Takahashi, K.A., and Castillo, P.E. (2006). Endocannabinoid-mediated synaptic plasticity in the CNS. Annu. Rev. Neurosci. *29*, 37–76.

Darios, F.E.D.E.R., Connell, E., and Davletov, B. (2007). Phospholipases and fatty acid signalling in exocytosis. J. Physiol. *585*, 699–704.

Dietrich, D., Kirschstein, T., Kukley, M., Pereverzev, A., von der Brelie, C., Schneider, T., and Beck, H. (2003). Functional specialization of presynaptic Cav2.3 Ca2+ channels. Neuron *39*, 483–496.

Fink, M., Lesage, F., Duprat, F., Heurteaux, C., Reyes, R., Fosset, M., and Lazdunski, M. (1998). A neuronal two P domain K+ channel stimulated by arachidonic acid and polyunsaturated fatty acids. EMBO J. *17*, 3297–3308.

Galimberti, I., Gogolla, N., Alberi, S., Santos, A.F., Muller, D., and Caroni, P. (2006). Long-term rearrangements of hippocampal mossy fiber terminal connectivity in the adult regulated by experience. Neuron *50*, 749–763.

Geiger, J.R.P., and Jonas, P. (2000). Dynamic control of presynaptic Ca(2+) inflow by fast-inactivating K(+) channels in hippocampal mossy fiber boutons. Neuron *28*, 927–939.

Gibson, H.E., Edwards, J.G., Page, R.S., Van Hook, M.J., and Kauer, J.A. (2008). TRPV1 channels mediate long-term depression at synapses on hippocampal interneurons. Neuron *57*, 746–759.

Hagen, V., Frings, S., Wiesner, B., Helm, S., Kaupp, U.B., and Bendig, J. (2003). [7-(Dialkylamino)coumarin-4-yl]methyl-Caged Compounds as Ultrafast and Effective Long-Wavelength Phototriggers of 8-Bromo-Substituted Cyclic Nucleotides. ChemBioChem *4*, 434–442.

Haj-Dahmane, S., and Shen, R.-Y. (2009). Endocannabinoids suppress excitatory synaptic transmission to dorsal raphe serotonin neurons through the activation of presynaptic CB1 receptors. J. Pharmacol. Exp. Ther. *331*, 186–196.

Hardie, R.C. (2007). TRP channels and lipids: from Drosophila to mammalian physiology. J. Physiol. *578*, 9–24.

Herkenham, M., Lynn, A.B., Little, M.D., Johnson, M.R., Melvin, L.S., de Costa, B.R., and Rice, K.C. (1990). Cannabinoid receptor localization in brain. Proc. Natl. Acad. Sci. USA *87*, 1932–1936.

Hofmann, M.E., Nahir, B., and Frazier, C.J. (2008). Excitatory afferents to CA3 pyramidal cells display differential sensitivity to CB1 dependent inhibition of synaptic transmission. Neuropharmacology 55, 1140–1146.

Isaac, J.T.R., Buchanan, K.A., Muller, R.U., and Mellor, J.R. (2009). Hippocampal place cell firing patterns can induce long-term synaptic plasticity in vitro. J. Neurosci. 29, 6840–6850.

Kamiya, H., Umeda, K., Ozawa, S., and Manabe, T. (2002). Presynaptic Ca2+ entry is unchanged during hippocampal mossy fiber long-term potentiation. J. Neurosci. 22, 10524–10528.

Kano, M., Ohno-Shosaku, T., Hashimotodani, Y., Uchigashima, M., and Watanabe, M. (2009). Endocannabinoid-mediated control of synaptic transmission. Physiol. Rev. 89, 309–380.

Katona, I., Urbán, G.M., Wallace, M., Ledent, C., Jung, K.M., Piomelli, D., Mackie, K., and Freund, T.F. (2006). Molecular composition of the endocannabinoid system at glutamatergic synapses. J. Neurosci. 26, 5628–5637.

Kawamura, Y., Fukaya, M., Maejima, T., Yoshida, T., Miura, E., Watanabe, M., Ohno-Shosaku, T., and Kano, M. (2006). The CB1 cannabinoid receptor is the major cannabinoid receptor at excitatory presynaptic sites in the hippocampus and cerebellum. J. Neurosci. 26, 2991–3001.

Kishimoto, K., Matsumura, K., Kataoka, Y., Morii, H., and Watanabe, Y. (1999). Localization of cytosolic phospholipase A2 messenger RNA mainly in neurons in the rat brain. Neuroscience 92, 1061–1077.

Kukkonen, J.P. (2011). A ménage à trois made in heaven: G-protein-coupled receptors, lipids and TRP channels. Cell Calcium 50, 9–26.

Lambeau, G., and Gelb, M.H. (2008). Biochemistry and physiology of mammalian secreted phospholipases A2. Annu. Rev. Biochem. 77, 495–520.

Lozovaya, N., Yatsenko, N., Beketov, A., Tsintsadze, T., and Burnashev, N. (2005). Glycine receptors in CNS neurons as a target for nonretrograde action of cannabinoids. J. Neurosci. 25, 7499–7506.

Ludwig, M., and Pittman, Q.J. (2003). Talking back: dendritic neurotransmitter release. Trends Neurosci. 26, 255–261.

Lüscher, C., Xia, H., Beattie, E.C., Carroll, R.C., von Zastrow, M., Malenka, R.C., and Nicoll, R.A. (1999). Role of AMPA receptor cycling in synaptic transmission and plasticity. Neuron 24, 649–658.

Marsicano, G., and Lutz, B. (2006). Neuromodulatory functions of the endocannabinoid system. J. Endocrinol. Invest. Suppl. 29, 27–46.

Mellor, J.R., and Nicoll, R.A. (2001). Hippocampal mossy fiber LTP is independent of postsynaptic calcium. Nat. Neurosci. 4, 125–126.

Meves, H. (2008). Arachidonic acid and ion channels: an update. Br. J. Pharmacol. 155, 4–16.

Nadler, A., Reither, G., Feng, S., Stein, F., Reither, S., Müller, R., and Schultz, C. (2013). The fatty acid composition of diacylglycerols determines local signaling patterns. Angew. Chem. Int. Ed. Engl. 52, 6330–6334.

Nicoll, R.A., and Schmitz, D. (2005). Synaptic plasticity at hippocampal mossy fibre synapses. Nat. Rev. Neurosci. 6, 863–876.

O'Dell, T.J., Hawkins, R.D., Kandel, E.R., and Arancio, O. (1991). Tests of the roles of two diffusible substances in long-term potentiation: evidence for nitric oxide as a possible early retrograde messenger. Proc. Natl. Acad. Sci. USA 88, 11285–11289.

Ohno-Shosaku, T., Tsubokawa, H., Mizushima, I., Yoneda, N., Zimmer, A., and Kano, M. (2002). Presynaptic cannabinoid sensitivity is a major determinant of depolarization-induced retrograde suppression at hippocampal synapses. J. Neurosci. 22, 3864–3872.

Oliver, D., Lien, C.-C., Soom, M., Baukrowitz, T., Jonas, P., and Fakler, B. (2004). Functional conversion between A-type and delayed rectifier K+ channels by membrane lipids. Science 304, 265–270.

Piomelli, D., Volterra, A., Dale, N., Siegelbaum, S.A., Kandel, E.R., Schwartz, J.H., and Belardetti, F. (1987). Lipoxygenase metabolites of arachidonic acid as second messengers for presynaptic inhibition of Aplysia sensory cells. Nature 328, 38–43.

Regehr, W.G., Carey, M.R., and Best, A.R. (2009). Activity-dependent regulation of synapses by retrograde messengers. Neuron 63, 154–170.

Roberts-Crowley, M.L., Mitra-Ganguli, T., Liu, L., and Rittenhouse, A.R. (2009). Regulation of voltage-gated Ca2+ channels by lipids. Cell Calcium 45, 589–601.

Ryberg, E., Larsson, N., Sjögren, S., Hjorth, S., Hermansson, N.-O., Leonova, J., Elebring, T., Nilsson, K., Drmota, T., and Greasley, P.J. (2007). The orphan receptor GPR55 is a novel cannabinoid receptor. Br. J. Pharmacol. 152, 1092–1101.

Sabatini, B.L., and Regehr, W.G. (1997). Control of neurotransmitter release by presynaptic waveform at the granule cell to Purkinje cell synapse. J. Neurosci. 17, 3425–3435.

Schaechter, J.D., and Benowitz, L.I. (1993). Activation of protein kinase C by arachidonic acid selectively enhances the phosphorylation of GAP-43 in nerve terminal membranes. J. Neurosci. 13, 4361–4371.

Sigel, E., Baur, R., Rácz, I., Marazzi, J., Smart, T.G., Zimmer, A., and Gertsch, J. (2011). The major central endocannabinoid directly acts at GABA(A) receptors. Proc. Natl. Acad. Sci. USA 108, 18150–18155.

Talbot, M.J., and Sayer, R.J. (1996). Intracellular QX-314 inhibits calcium currents in hippocampal CA1 pyramidal neurons. J. Neurophysiol. 76, 2120–2124.

Tanimura, A., Yamazaki, M., Hashimotodani, Y., Uchigashima, M., Kawata, S., Abe, M., Kita, Y., Hashimoto, K., Shimizu, T., Watanabe, M., et al. (2010). The endocannabinoid 2-arachidonoylglycerol produced by diacylglycerol lipase alpha mediates retrograde suppression of synaptic transmission. Neuron 65, 320–327.

Trimbuch, T., Beed, P., Vogt, J., Schuchmann, S., Maier, N., Kintscher, M., Breustedt, J., Schuelke, M., Streu, N., Kieselmann, O., et al. (2009). Synaptic PRG-1 modulates excitatory transmission via lipid phosphate-mediated signaling. Cell 138, 1222–1235.

Vaidyanathan, V.V., Yoshino, K., Jahnz, M., Dörries, C., Bade, S., Nauenburg, S., Niemann, H., and Binz, T. (1999). Proteolysis of SNAP-25 isoforms by botulinum neurotoxin types A, C, and E: domains and amino acid residues controlling the formation of enzyme-substrate complexes and cleavage. J. Neurochem. 72, 327–337.

Villacres, E.C., Wong, S.T., Chavkin, C., and Storm, D.R. (1998). Type I adenylyl cyclase mutant mice have impaired mossy fiber long-term potentiation. J. Neurosci. 18, 3186–3194.

Villarroel, A., and Schwarz, T.L. (1996). Inhibition of the Kv4 (Shal) family of transient K+ currents by arachidonic acid. J. Neurosci. 16, 2522–2532.

Wang, H., Pineda, V.V., Chan, G.C.K., Wong, S.T., Muglia, L.J., and Storm, D.R. (2003). Type 8 adenylyl cyclase is targeted to excitatory synapses and required for mossy fiber long-term potentiation. J. Neurosci. 23, 9710–9718.

Williams, J.H., Errington, M.L., Lynch, M.A., and Bliss, T.V.P. (1989). Arachidonic acid induces a long-term activity-dependent enhancement of synaptic transmission in the hippocampus. Nature 341, 739–742.

Wilson, R.I., and Nicoll, R.A. (2002). Endocannabinoid signaling in the brain. Science 296, 678–682.

Yeckel, M.F., Kapur, A., and Johnston, D. (1999). Multiple forms of LTP in hippocampal CA3 neurons use a common postsynaptic mechanism. Nat. Neurosci. 2, 625–633.